Richter, MJ, Wagmann, L, Kavanagh, PV, Brandt, SD and Meyer, MR

 In vitro metabolic fate of the synthetic cannabinoid receptor agonists QMMSB (quinolin-8-yl 4-methyl-3-(morpholine-4-sulfonyl)benzoate) and QMiPSB (quinolin-8-yl 4-methyl-3-[(propan-2-yl)sulfamoyl]benzoate) including isozyme mapping and carboxylesterases activity testing

https://researchonline.ljmu.ac.uk/id/eprint/17838/

Article

RESEARCH ARTICLE

WILEY

In vitro metabolic fate of the synthetic cannabinoid receptor agonists (quinolin-8-yl 4-methyl-3-(morpholine-4-sulfonyl)benzoate [QMMSB]) and (quinolin-8-yl 4-methyl-3-((propan-2-yl)sulfamoyl)benzoate [QMiPSB]) including isozyme mapping and carboxylesterases activity testing

Matthias J. Richter[1] | Lea Wagmann[1] | Pierce V. Kavanagh[2] |
Simon D. Brandt[3] | Markus R. Meyer[1]

[1]Department of Experimental and Clinical Toxicology, Institute of Experimental and Clinical Pharmacology and Toxicology, Center for Molecular Signaling (PZMS), Saarland University, Homburg, Germany

[2]Department of Pharmacology and Therapeutics, School of Medicine, Trinity Centre for Health Sciences, St. James Hospital, Dublin 8, Ireland

[3]School of Pharmacy and Biomolecular Sciences, Liverpool John Moores University, Liverpool, UK

Correspondence
Markus R. Meyer, Department of Experimental and Clinical Toxicology, Institute of Experimental and Clinical Pharmacology and Toxicology, Center for Molecular Signaling (PZMS), Saarland University, Homburg, Germany.
Email: m.r.meyer@mx.uni-saarland.de

Abstract

The synthetic cannabinoid receptor agonists (SCRAs) (quinolin-8-yl 4-methyl-3-(morpholine-4-sulfonyl)benzoate [QMMSB]) and (quinolin-8-yl 4-methyl-3-((propan-2-yl)sulfamoyl)benzoate [QMiPSB], also known as SGT-46) are based on the structure of quinolin-8-yl 4-methyl-3-(piperidine-1-sulfonyl)benzoate (QMPSB) that has been identified on seized plant material in 2011. In clinical toxicology, knowledge of the metabolic fate is important for their identification in biosamples. Therefore, the aim of this study was the identification of in vitro Phase I and II metabolites of QMMSB and QMiPSB in pooled human liver S9 fraction (pHLS9) incubations for use as screening targets. In addition, the involvement of human monooxygenases and human carboxylesterases (hCES) was examined. Analyses were performed by liquid chromatography coupled with high-resolution tandem mass spectrometry. Ester hydrolysis was found to be an important step in the Phase I metabolism of both SCRAs, with the carboxylic acid product being found only in negative ionization mode. Monohydroxy and N-dealkyl metabolites of the ester hydrolysis products were detected as well as glucuronides. CYP2C8, CYP2C9, CYP3A4, and CYP3A5 were involved in hydroxylation. Whereas enzymatic ester hydrolysis of QMiPSB was mainly catalyzed by hCES1 isoforms, nonenzymatic ester hydrolysis was also observed. The results suggest that ester hydrolysis products of QMMSB and QMiPSB and their glucuronides are suitable targets for toxicological screenings. The additional use of the negative ionization mode is recommended to increase detectability of analytes. Different cytochrome P450 (CYP) isozymes were involved in the metabolism; thus, the probability of drug–drug interactions due to CYP inhibition can be assessed as low.

1 | INTRODUCTION

Synthetic cannabinoids, also referred as synthetic cannabinoid receptor agonists (SCRAs), represent one of the largest subgroups of new psychoactive substances (NPS).[1] SCRAs can cause severe poisoning and even death.[2] Each year, over 100 different SCRAs are identified on drug markets around the world.[1] The chemical structures are modified to circumvent legislation or optimize potency so that new substances are continuously introduced.[1] In 2021, 15 new SCRAs were reported for the first time in Europe.[3] SCRAs are often sprayed on plant material and sold as "herbal smoking mixtures."[4]

In 2007, quinolin-8-yl 4-methyl-3-(piperidine-1-sulfonyl)benzoate (QMPSB) (Figure 1) was discovered during high-throughput screening as a potent SCRA. Subsequently, QMPSB became a template for a group of SCRAs containing a sulfamoyl benzoate core and/or a quinolin-8-yl ester head group.[5] Previous research showed that QMPSB acts as an agonist at the cannabinoid receptors CB1 and CB2, with moderate selectivity for the CB2 receptor.[5,6] QMPSB derivatives were screened in search of structures with improved potency, receptor selectivity, and chemical stability. However, all examined derivatives showed reduced potency at the CB1 receptor, whereby the CB1 potency of the morpholine analog quinolin-8-yl 4-methyl-3-(morpholine-4-sulfonyl) benzoate (QMMSB) was only slightly lower (Figure 1).[5] In 2012, a company started working on this group of SCRAs to develop substances for therapeutic applications. In trials on human volunteers, QMPSB and QMMSB were found to be psychoactive, even though the effect seemed to be of short duration.[7] It was also reported that both substances had poor solubility and thermal instability.[7] Various QMPSB derivatives were studied, including QMiPSB (also known as SGT-46), which has an isopropyl tail group instead of the piperidine ring (Figure 1). However, QMiPSB showed reduced potency compared to QMPSB.[7] After the chemical structures became known, QMPSB appeared on the NPS market in Australia in

2011,[8] and its difluoro derivative 2F-QMPSB appeared in Italy in 2018.[9] The combination of the quinolin-8-yl ester head group of QMPSB with an N-alkyl-1H-indole core led to the SCRAs PB-22 (also known as QUPIC) and BB-22 (also known as QUCHIC), which appeared on the NPS market in 2012 and 2013 for the first time.[10]

For clinical and forensic toxicology, metabolism data of emerging NPS are needed to develop screening methods, particularly for plasma and urine samples. For many SCRAs, only metabolites can usually be found in urine, but not the parent compound.[11] To our knowledge, no data on the metabolism of QMMSB and QMiPSB are available in the literature. Therefore, this study was designed to identify metabolites of these two SCRAs to serve as potential targets for toxicological screening approaches using liquid chromatography coupled to high-resolution tandem mass spectrometry (LC-HR-MS/MS). In vitro incubations with pooled human liver S9 fraction (pHLS9) were used for the identification of Phase I and II metabolites. In addition, the involvement of individual monooxygenases in the Phase I metabolism was examined using an in vitro monooxygenase screening procedure. Since earlier studies showed that human carboxylesterases (hCES) are involved in the metabolism of related SCRAs with a quinolin-8-yl ester head group, a carboxylesterases activity assay was also performed.[12,13]

2 | EXPERIMENTAL

2.1 | Chemicals and reagents

QMMSB and QMiPSB were provided by Stargate International (Auckland, New Zealand) and were available from previous studies.[7] Stock solutions of QMMSB and QMiPSB were prepared in acetonitrile (1 mg/ml) and were stored at −18°C. Trimipramine-d$_3$ and glibenclamide were bought from LGC Standards (Wesel, Germany). Isocitrate, isocitrate dehydrogenase (IDH), superoxide dismutase (SOD), 3′-phosphoadenosine-5′-phosphosulfate (PAPS), S-(5′-adenosyl)-L-methionine (SAM), dithiothreitol, reduced glutathione, magnesium chloride (MgCl$_2$), potassium dihydrogen phosphate (KH$_2$PO$_4$), dipotassium hydrogen phosphate (K$_2$HPO$_4$), and tris(hydroxymethyl)aminomethane hydrochloride were bought from Sigma-Aldrich (Taufkirchen, Germany). Nicotinamide adenine dinucleotide phosphate (NADP$^+$) was purchased at Biomol (Hamburg, Germany). Baculovirus-infected insect cell microsomes (Supersomes) containing the human complementary DNA-expressed cytochrome P450 (CYP) isozymes CYP1A2 (1 nmol/ml), CYP2A6 (2 nmol/ml), CYP2B6 (1 nmol/ml), CYP2C8 (1 nmol/ml), CYP2C9 (2 nmol/ml), CYP2C19 (1 nmol/ml), CYP2D6 (1 nmol/ml), CYP2E1 (2 nmol/ml), CYP3A4 (1 nmol/ml), and CYP3A5 (1 nmol/ml); flavin-containing monooxygenase 3 (FMO3, 5 mg/ml); recombinant hCES1b (5 mg/ml), hCES1c (5 mg/ml), and
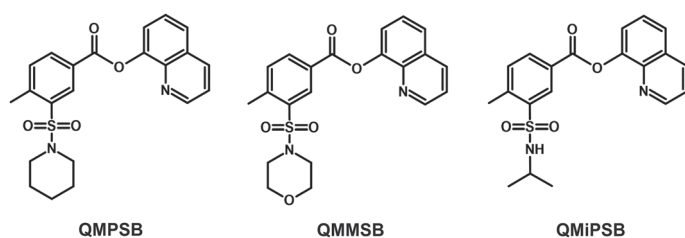

FIGURE 1 Chemical structures of the template compound quinolin-8-yl 4-methyl-3-(piperidine-1-sulfonyl)benzoate (QMPSB) and the two examined synthetic cannabinoid receptor agonists (SCRAs) quinolin-8-yl 4-methyl-3-(morpholine-4-sulfonyl)benzoate (QMMSB) and quinolin-8-yl 4-methyl-3-((propan-2-yl)sulfamoyl) benzoate (QMiPSB)

hCES2 (5 mg/ml); pooled human liver microsomes (pHLM, 20 mg protein/mL, 360 pmol total CYP/mg, 26 donors) and pHLS9 (20 mg protein/mL, 8 donors); and UGT reaction mixture solution A (25mM UDP-glucuronic acid) and UGT reaction mixture solution B (250mM Tris HCl, 40mM $MgCl_2$, and 125 μg alamethicin/mL) were bought from Corning (Amsterdam, the Netherlands). Sufficient activities of the enzymes used (IDH, SOD, CYP, FMO3, hCES, pHLM, and pHLS9) were shown by the manufacturers using suitable test substrates. The enzymes were thawed at 37°C after delivery, aliquoted, snap-frozen in liquid nitrogen, and stored at −80°C until use. Acetonitrile (LC–MS grade), methanol (LC–MS grade), ammonium formate (analytical grade), formic acid (LC–MS grade), and all other reagents and chemicals (analytical grade) were bought from VWR (Darmstadt, Germany).

2.2 | Investigation of Phase I and II metabolites using pHLS9 incubations

The incubations of QMMSB or QMiPSB with pHLS9 were performed according to a previous publication with the following minor modifications.[14] The acetyl coenzyme A system was omitted since acetylation was not suspected to be the main metabolic pathway of the investigated substances. Both substances were incubated with pHLS9 for 6 h, with a 60 μl sample taken after 1 h. Trimipramine-d_3 (2.5 μM) was chosen as internal standard (IS).

2.3 | Monooxygenases activity screening

QMMSB and QMiPSB were incubated with 11 different recombinant monooxygenases for 30 min according to a protocol employed previously with minor modifications.[15] The concentration of trimipramine-d_3 as IS was reduced to 2.5 μM, and the samples were centrifuged at 18,407 ×g for 2 min after the incubation.

2.4 | Carboxylesterases activity screening

QMMSB and QMiPSB were incubated with recombinant hCES1b, hCES1c, and hCES2 as well as with pHLM and pHLS9 for 60 min according to the protocol used in a previous study.[13]

2.5 | LC-HRMS/MS settings

LC-HR-MS/MS analysis of all experiments was performed with a Thermo Fisher Scientific (TF, Dreieich, Germany) Dionex UltiMate 3000 RS LC system consisting of a degasser, a quaternary pump, and an HTC PAL Autosampler (CTC Analytics AG, Zwingen, Switzerland) coupled to a TF Q-Exactive mass spectrometer with a heated electrospray ionization (HESI)-II source. External mass calibration was performed before analysis. The injection volume of the samples was set to 5 μl. A TF Accucore Phenyl-Hexyl column (100 mm × 2.1 mm,

2.6 μm) was used with a gradient elution at 40°C as described in a previous publication.[16] The HESI-II settings from an earlier publication were used, with a separate run being performed in negative ionization mode in addition to positive ionization.[17] Mass spectrometer settings and subsequent data analysis were carried out according to a method described previously, with the scan range for the expected metabolites of QMMSB and QMiPSB set to a mass-to-charge ratio (m/z) 80–850.[17] Deviations between measured and calculated precursor ion (PI) masses were determined, and a maximum deviation of 5 ppm was tolerated. In case of fragment ions (FIs), ppm deviations of more than 5 ppm were acceptable. FIs at low m/z (<100) measured in negative ionization mode often show deviations above 5 ppm.

3 | RESULTS AND DISCUSSION

3.1 | Identification of in vitro Phase I and II metabolites of QMMSB

Exact protonated and deprotonated PI masses of expected Phase I and II metabolites were calculated. High-resolution (HR) full scan data from the pHLS9 and monooxygenase isozyme incubations were screened for the calculated PI masses, and the corresponding MS^2 spectra were interpreted. All metabolites could only be tentatively identified as no reference materials were available.

Eleven Phase I and four Phase II metabolites of QMMSB were detected in pHLS9 and/or monooxygenase isozyme incubations (metabolites MM1–MM15; see Table S1 in the Electronic Supplementary Material, ESM). Table S1 also contains the ionization mode (positive or negative) and incubation type (pHLS9 and/or monooxygenase isozyme incubation) in which the respective metabolites were detected.

Seven metabolites were detected in pHLS9 incubations. No metabolite with an intact ester moiety could be found, which is consistent with previous studies on the related SCRAs QMPSB, QMPCB, and 2F-QMPSB.[12,13] All detected metabolites were ester hydrolysis products or metabolites thereof. In accordance with previous studies on related SCRAs, the ester hydrolysis products MM6 and MM11 (Table S1) could be found in the control samples without enzyme, which suggests nonenzymatic ester hydrolysis.[12,13] The 1-h and 6-h samples of pHLS9 incubations showed the same QMMSB metabolites.

The MS^2 spectra of QMMSB and its most abundant metabolites in pHLS9 incubations are depicted in Figure 2a–f. MS^2 spectra of additional metabolites are shown in Figure S1 (ESM). The MS^2 spectrum of QMMSB (Figure 2a/Table S1) with the protonated PI at m/z 413.1166 ($C_{21}H_{21}N_2O_5S$) is in accordance with a previous publication.[7] The base peak at m/z 286.0744 ($C_{12}H_{16}NO_5S$) results from the loss of the quinoline head group. Further cleavage of the morpholine ring leads to the FI at m/z 183.0110 ($C_8H_7O_3S$). Further elimination of SO_2 and CO leads to the FIs at m/z 119.0491 (C_8H_7O) and m/z 91.0542 (C_7H_7). Metabolite MM6 (Figure 2b/Table S1) is the carboxylic acid product of ester hydrolysis with the deprotonated PI at m/z

(a) MS² of QMMSB (*m/z* at 413.1166, RT 8.6 min, pos)

(b) MS² of MM6 (ester hydrolysis: carboxylic acid, *m/z* at 284.0598, RT 6.8 min, neg)

(c) MS² of MM10 (ester hydrolysis: carboxylic acid + gluc, *m/z* at 460.0919, RT 6.0 min, neg)

(d) MS² of MM11 (ester hydrolysis: 8-hydroxyquinoline, *m/z* at 146.0600, RT 2.2 min, pos)

(e) MS² of MM14 (ester hydrolysis: 8-hydroxyquinoline + gluc, *m/z* at 322.0921, RT 1.6 min, pos)

(f) MS² of MM15 (ester hydrolysis: 8-hydroxyquinoline + monohydroxy + gluc, *m/z* at 338.0870, RT 1.4 min, pos)

FIGURE 2   Legend on next page.

284.0598 ($C_{12}H_{14}NO_5S$). Loss of CO_2 and the 4-methyl benzoate core results in the FI at m/z 240.0700 ($C_{11}H_{14}NO_3S$) and m/z 150.0230 ($C_4H_8NO_3S$). Metabolite MM10 (Figure 2c/Table S1) with the PI at m/z 460.0919 ($C_{18}H_{22}NO_{11}S$) is the glucuronide of the ester hydrolysis product MM6. The loss of glucuronic acid, CO_2, and the 4-methyl benzoate core leads to the FI at m/z 284.0598 ($C_{12}H_{14}NO_5S$), m/z 240.0700 ($C_{11}H_{14}NO_3S$), and m/z 150.0230 ($C_4H_8NO_3S$), which were also present in the MS^2 spectrum of MM6. Metabolite MM11 (Figure 2d/Table S1) is the ester hydrolysis product 8-hydroxyquinoline with the protonated PI at m/z 146.0600 (C_9H_8NO). Loss of CO results in the FI at m/z 118.0651 (C_8H_8N). Metabolite MM14 (Figure 2e/Table S1) is the glucuronidated 8-hydroxyquinoline with the protonated PI at m/z 322.0921 ($C_{15}H_{16}NO_7$). Loss of glucuronic acid leads to the FI at m/z 146.0600 (C_9H_8NO), which corresponds to the protonated PI of MM11. The hydroxylated and glucuronidated 8-hydroxyquinoline with the protonated PI at m/z 338.0870 ($C_{15}H_{16}NO_8$) (metabolite MM15 in Figure 2f/Table S1) was also detected. After cleavage of the glucuronic acid, the hydroxylated 8-hydroxyquinoline with FI at m/z 162.0550 ($C_9H_8NO_2$) is formed.

In previous studies on the related cannabinoids QMPSB and 2F-QMPSB, the carboxylic acid products of ester hydrolysis and metabolites thereof either were only detectable in the negative ionization mode or had only a higher abundance compared to measurements in the positive mode.[12,13] Therefore, the negative ionization mode was also used in this study. In fact, QMMSB metabolites derived from the carboxylic acid product of ester hydrolysis could only be measured in the negative ionization mode (MM7–MM9 in Table S1) or had a higher abundance in the negative ionization mode (MM6 and MM10 in Table S1). Consequently, a combination of positive and negative ionization modes increases the detectability of QMMSB metabolites and provides opportunities to confirm the results obtained in the positive mode.

3.2 | Identification of in vitro Phase I and II metabolites of QMiPSB

Twelve Phase I and four Phase II QMiPSB metabolites have been tentatively identified in pHLS9 and/or monooxygenase isozyme incubations (metabolites IM1–IM16 in Table S2). Table S2 shows the ionization mode used and the incubation type in which the metabolites were detected.

Eight QMiPSB metabolites were detected in pHLS9 incubations (Table S2). Comparable to the QMMSB results, no metabolite identified in the pHLS9 incubation had an intact ester group. The ester hydrolysis products of QMiPSB could also be detected in the control sample, indicating nonenzymatic ester hydrolysis.

Figure 3a–f depicts the MS^2 spectra of QMiPSB and its most abundant metabolites in pHLS9 incubations. MS^2 spectra of further QMiPSB metabolites can be found in Figure S2. The MS^2 spectrum of QMiPSB (Figure 3a/Table S2) with the protonated PI at m/z 385.1217 ($C_{20}H_{21}N_2O_4S$) is comparable to data of a previous publication.[7] Loss of the 8-hydroxyquinoline head group leads to the base peak at m/z 240.0689 ($C_{11}H_{14}NO_3S$). Loss of the isopropyl group, SO_2, and CO resulted in the FI at m/z 183.0110 ($C_8H_7O_3S$), m/z 119.0491 (C_8H_7O), and m/z 91.0542 (C_7H_7). Metabolite IM7 (Figure 3b/Table S2) is the carboxylic acid product of ester hydrolysi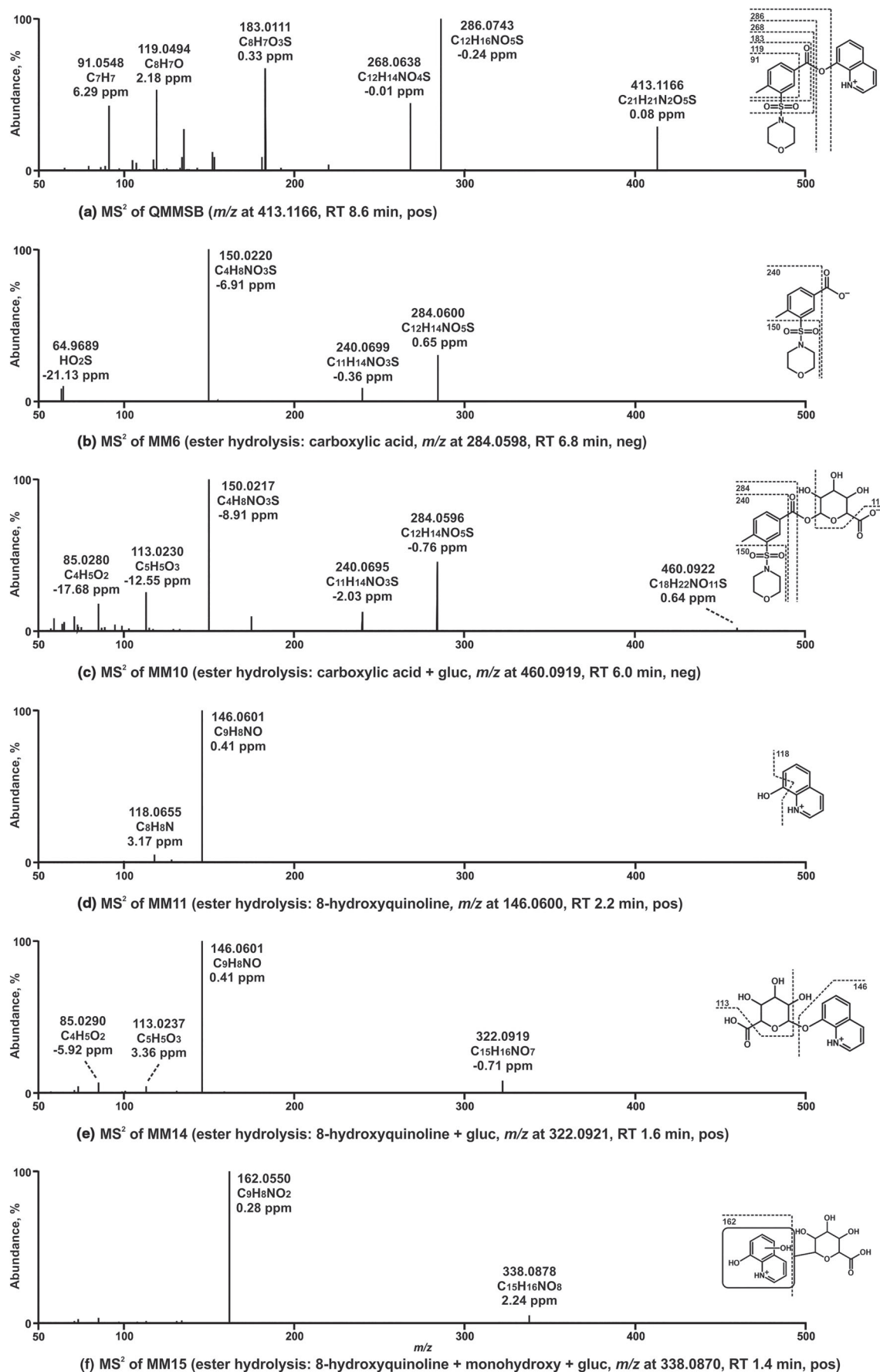s with the deprotonated PI at m/z 256.0649 ($C_{11}H_{14}NO_4S$). Cleavage of CO_2 and the 4-methyl benzoate core leads to the FI at m/z 212.0751 ($C_{10}H_{14}NO_2S$) and m/z 122.0281 ($C_3H_8NO_2S$). Metabolite IM10 (Figure 3c/Table S2) is the glucuronide of IM7 with the deprotonated PI at m/z 432.0970 ($C_{17}H_{22}NO_{10}S$). Loss of glucuronic acid, CO_2, and the 4-methyl benzoate core leads to the FIs at m/z 256.0649 ($C_{11}H_{14}NO_4S$), m/z 212.0751 ($C_{10}H_{14}NO_2S$), and m/z 122.0281 ($C_3H_8NO_2S$), which are also the characteristic ions in the MS^2 spectra of the non-glucuronidated metabolite IM7. Metabolite IM11 (Figure 3d/Table S2) is the ester hydrolysis product 8-hydroxyquinoline. Both QMMSB and QMiPSB bear an 8-hydroxyquinoline ester head group and thus share similar metabolites. The MS^2 spectrum of 8-hydroxyquinoline, its glucuronide, and the hydroxylated and glucuronidated 8-hydroxyquinoline (IM11, IM15, and IM16 in Figure 3d–f) were discussed above as metabolites of QMMSB (MM11, MM14, and MM15 in Figure 2d–f).

In agreement with the results of QMMSB, the additional use of the negative ionization mode could also increase the detectability of QMiPSB metabolites. Metabolites of the carboxylic acid product after ester hydrolysis could only be measured in the negative ionization mode (IM8–IM10 in Table S2). The carboxylic acid product itself was found with a higher abundance in the negative ionization mode compared to the positive ionization mode (IM7 in Table S2). Therefore, when developing bioanalytical methods for QMiPSB, a combination of positive and negative ionization mode is recommended to increase detectability of the metabolites.

3.3 | Proposed metabolic pathways of QMMSB

The proposed metabolic pathways of QMMSB are shown in Figure 4. In accordance with previous studies on related SCRAs, which also carry an 8-hydroxyquinoline ester head group, ester hydrolysis was also an important step in the metabolism of QMMSB.[12,13] Therefore, the metabolites of QMMSB were divided into three groups: metabolites with an intact ester group (MM1–MM5 in Figure 4), the carboxylic acid product after ester hydrolysis with additional metabolic reactions (MM6–MM10 in Figure 4), and the ester hydrolysis product
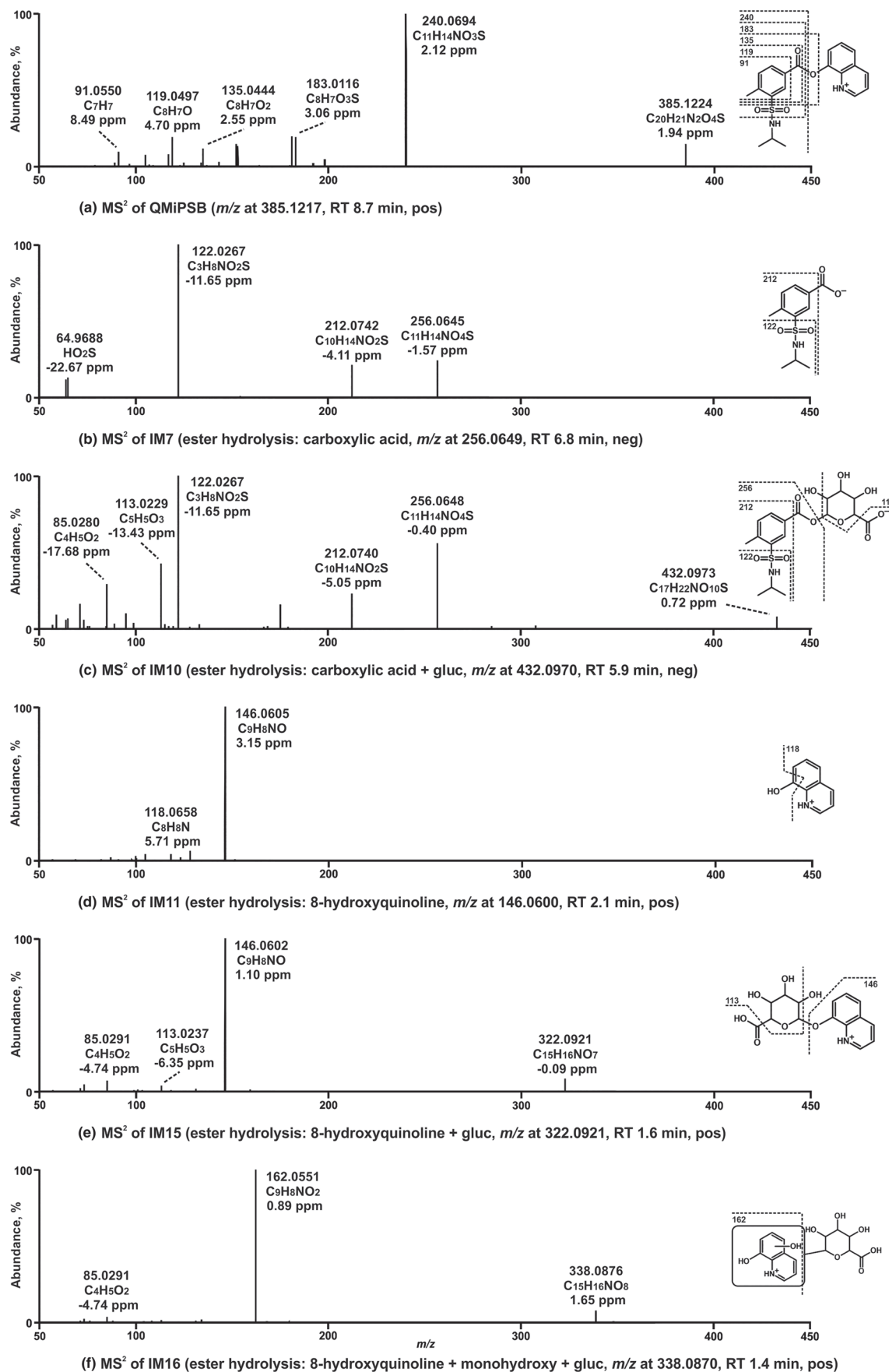
(a) MS² of QMiPSB (*m/z* at 385.1217, RT 8.7 min, pos)

(b) MS² of IM7 (ester hydrolysis: carboxylic acid, *m/z* at 256.0649, RT 6.8 min, neg)

(c) MS² of IM10 (ester hydrolysis: carboxylic acid + gluc, *m/z* at 432.0970, RT 5.9 min, neg)

(d) MS² of IM11 (ester hydrolysis: 8-hydroxyquinoline, *m/z* at 146.0600, RT 2.1 min, pos)

(e) MS² of IM15 (ester hydrolysis: 8-hydroxyquinoline + gluc, *m/z* at 322.0921, RT 1.6 min, pos)

(f) MS² of IM16 (ester hydrolysis: 8-hydroxyquinoline + monohydroxy + gluc, *m/z* at 338.0870, RT 1.4 min, pos)

FIGURE 3   Legend on next page.

FIGURE 3   HR-MS^2 spectra of quinolin-8-yl 4-methyl-3-((propan-2-yl)sulfamoyl)benzoate (QMiPSB) and most abundant QMiPSB metabolites detected in pooled human liver S9 fraction (pHLS9) incubations (IM7, IM10, IM11, IM15, and IM16). gluc, glucuronic acid; neg, negative ionization mode; pos, positive ionization mode; RT, retention time
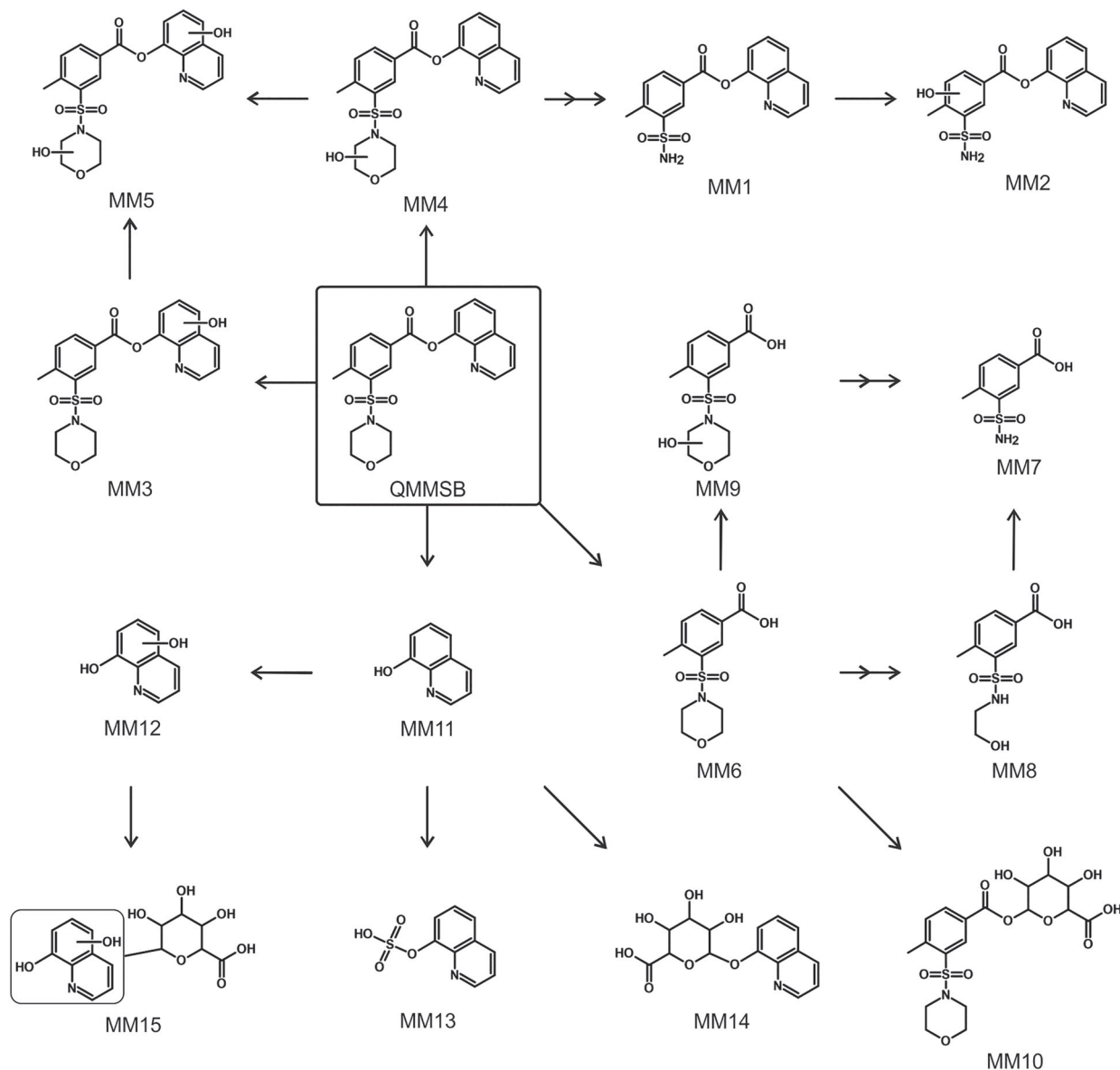

FIGURE 4   Proposed in vitro metabolic pathways of quinolin-8-yl 4-methyl-3-(morpholine-4-sulfonyl)benzoate (QMMSB). gluc, glucuronic acid; MM1–MM15, metabolites of QMMSB

8-hydroxyquinoline with additional metabolic reactions (MM11–MM15 in Figure 4).

All metabolites with an intact ester linker (MM1–MM5 in Figure 4) and MM7, MM8, and MM12 (Figure 4) were only detected in some of the monooxygenase isozyme incubations but not in pHLS9 incubations. As hCES are naturally contained in the pHLS9 fraction and the incubation time for the pHLS9 experiments was even longer than the monooxygenase isozyme incubations, this might result in the observed extensive ester hydrolysis. Furthermore, the formed Phase I metabolites in pHLS9 incubations could

have been further metabolized to Phase II metabolites, following the missing detection of Phase I metabolites. Therefore, metabolites detected in the pHLS9 incubations should reflect the in vivo situation more accurately, as opposed to the additional Phase I metabolites only found in the monooxygenase incubations. In vivo data are available in the literature for the related SCRA FUB-PB-22, which also has a quinolin-8-yl ester head group but an N-alkyl-1H-indole core instead of a sulfamoyl benzoate core. Neither the parent compound nor the metabolites with an intact ester bond could be detected in an authentic urine sample.[18]

MM6 (Figure 4) is the carboxylic acid product of ester hydrolysis. Hydroxylation of the morpholine ring of MM6 resulted in metabolite MM9. Based on the MS^2 spectrum alone, the position of the hydroxy group cannot be determined with certainty but can be narrowed down to certain parts of the molecule, such as the morpholine ring in the case of MM9. Therefore, MM9 can also be hydroxylated in the α-position next to the nitrogen atom of the morpholine ring, which can lead to ring opening. This mechanism has already been described for other substances.[19,20] Further metabolic steps resulted in the cleavage of one C2 alkyl chain of the morpholine ring (MM8; *N,O*-bis-dealkylation) or both C2 alkyl chains of the morpholine ring (MM7; *N,N*-bis-dealkylation). Glucuronidation of the carboxylic acid product MM6 led to the acyl glucuronide MM10.

The ester hydrolysis product 8-hydroxyquinoline (MM11) was hydroxylated to MM12 (Figure 4). In Phase II metabolism, the glucuronides of MM11 and MM12 were detected (MM14 and MM15). Sulfation of 8-hydroxyquinoline formed metabolite MM13.

Five metabolites with an intact ester group could be detected (MM1–MM5 in Figure 4). Monohydroxylation on the quinoline head group or the morpholine ring led to MM3 and MM4. The dihydroxy metabolite MM5 is hydroxylated at both the quinoline head group and the morpholine ring. MM1 is the *N,N*-bis-dealkyl metabolite, which was hydroxylated on the 4-methyl benzoate core, resulting in MM2.

In comparison with an earlier in vitro study on the SCRA QMPSB, which carries a piperidine ring instead of a morpholine ring, a large number of similar metabolites were found[12]: The metabolites MM1, MM7, and MM11–MM14 were also identified in QMPSB incubations since these do not contain the piperidine or morpholine tail structure. In the case of the metabolites MM3, MM5, MM6, MM9, and MM10 containing the morpholine structure, the analogous metabolites with a piperidine ring were formed in the QMPSB incubations. Moreover, in the QMPSB incubations, further metabolites could be identified, which show hydroxylation steps on the piperidine ring, since the piperidine ring has more potential positions available for hydroxylation compared to the morpholine ring.

From the seven metabolites identified in the pHLS9 incubations, the ester hydrolysis products MM6 and MM11 and their glucuronides MM10 and MM14 had the most abundant signals. Hence, these metabolites should be treated as the main targets for toxicological screenings. Published in vivo data from the related SCRA FUB-PB-22 describe the acyl glucuronide of the ester hydrolysis product as the major metabolite in an authentic urine specimen.[18] Furthermore, it is important to note that various SCRAs carry an 8-hydroxyquinoline ester head group. Considering this, 8-hydroxyquinoline and its metabolites are not specific metabolites of QMMSB, but they can indicate the presence of an SCRA with this head group.

3.4 | Proposed metabolic pathways of QMiPSB

The proposed metabolic pathways of QMiPSB are depicted in Figure 5. The structures of QMMSB and QMiPSB differ only in the tail group, resulting in the detection of similar metabolic steps. Thus, ester hydrolysis also played an important role in the metabolism of QMiPSB: The metabolites IM1–IM6 have an intact ester group, IM7–IM10 are the carboxylic acid product of ester hydrolysis or its metabolites, and IM11–IM16 are the ester hydrolysis product 8-hydroxyquinoline or its metabolites.

The carboxylic acid product of the ester hydrolysis IM7 (Figure 5), its acyl glucuronide IM10, and the *N*-dealkyl metabolite IM8 were formed. Furthermore, the monohydroxy metabolite IM9 was identified, whereby the exact position of the hydroxy group on the core structure could not be specified based on the fragmentation. Metabolites IM12 and IM14–IM16 were also identified in incubations with QMMSB derived from the 8-hydroxyquinoline structure (IM11). Only the dihydroxy metabolite IM13 could be detected as an additional metabolite in the QMiPSB incubations. Among the metabolites with an intact ester bond, three monohydroxy isomers IM3–IM5 could be detected, sharing the same fragmentation pattern. Retention times vary slightly, indicating different hydroxylation positions on the quinoline structure. Furthermore, the *N*-dealkyl metabolite IM1 and its monohydroxy metabolite IM2 were detected, which were also identified as metabolites of QMMSB (MM1 and MM2).

Comparable to QMMSB, in the pHLS9 incubations with QMiPSB, the two ester hydrolysis products IM7 and IM11 as well as their glucuronides IM10 and IM15 had the most abundant signals (Figure 5). Therefore, these metabolites should be regarded as the main targets for toxicological screenings.

3.5 | Monooxygenases activity screening

Several monooxygenases contributed to the Phase I metabolism of QMMSB and QMiPSB (Tables S3 and S4). Both SCRAs were metabolized by CYP2C8, CYP2C9, CYP3A4, and CYP3A5. In addition, CYP2C19 also played an important role in the metabolism of QMMSB, whereas CYP1A2 was involved in the metabolism of QMiPSB. Since both SCRAs are metabolized via several monooxygenases, they can be further degraded if a single CYP enzyme is inhibited. Hence, a drug–drug interaction due to inhibition of a single CYP isozyme seems to be unlikely. The same can be expected from a person with a poor metabolizer status for a single CYP isozyme.[15] The ester hydrolysis products of both SCRAs were found in all enzyme incubations (CYP isozymes, FMO3, and HLM) but also in the control incubations, so that they appear to be formed by nonenzymatic degradation.

3.6 | Carboxylesterases activity screening of QMiPSB

Rapid ester hydrolysis of the quinolin-8-yl ester head groups of QMMSB and QMiPSB was revealed in the pHLS9 incubations. Previous studies describe the instability of this SCRA head group in the form of hydrolysis and transesterification with solvents like methanol
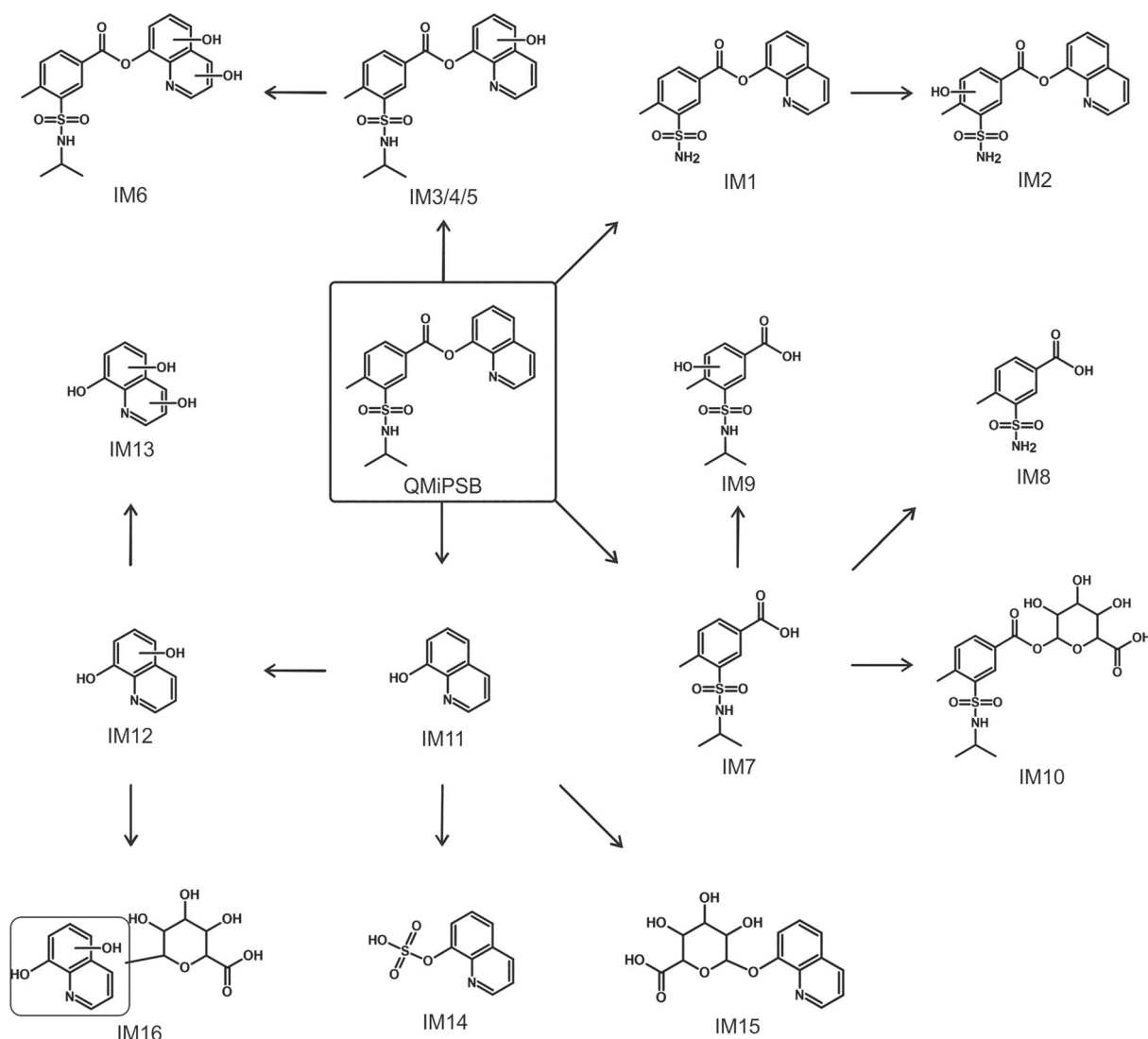
FIGURE 5 Proposed in vitro metabolic pathways of quinolin-8-yl 4-methyl-3-((propan-2-yl)sulfamoyl)benzoate (QMiPSB). gluc, glucuronic acid; IM1–IM16, metabolites of QMiPSB

or ethanol.[6,8] A carboxylesterases activity screening was also employed to assess the influence of different hCES on the metabolism of the investigated SCRA. However, this assay could only be performed for QMiPSB as not enough parent compound of QMMSB was available.

The hydrolysis of many ester-containing endogenous and exogenous substances is catalyzed by hCES, with the isoforms hCES1b and hCES1c being expressed primarily in the lung and in the liver and hCES2 in the gastrointestinal tract.[21–24] Therefore, QMiPSB was incubated with the recombinant isoforms hCES1b, hCES1c, and hCES2 as well as with pHLM and pHLS9, which represent the diversity of natural carboxylesterases in the human liver. Furthermore, control samples without enzymes were also prepared, since earlier studies on the related SCRAs QMPSB, QMPCB, and 2F-QMPSB have shown nonenzymatic ester hydrolysis.[12,13]

The ester hydrolysis of QMiPSB was monitored via the peak area of the carboxylic acid hydrolysis product (IM7 in Figure 5). Samples

were taken after 0, 8, 14, 20, 30, and 45 min. The peak area of the carboxylic acid product of the 0 min sample was subtracted from the other samples to capture only ester hydrolysis during the incubation period. The incubations were performed in duplicates. The mean values of the duplicates are displayed in Figure 6. In the control incubations, an increase in the carboxylic acid product IM7 could be detected because of nonenzymatic ester hydrolysis, since the control incubations did not contain any carboxylesterases. This observation agrees with previous studies on related SCRAs with a quinolin-8-yl ester head group, which also showed nonenzymatic ester hydrolysis.[12,13] The incubations with hCES showed a faster increase of the ester hydrolysis product IM7 compared to the control samples, indicating enzymatic hydrolysis. The ester hydrolysis product increased faster in the incubations with hCES1b and hCES1c than in the incubations with hCES2. The ester bond of QMiPSB thus appears to be predominantly cleaved by hCES1 isoforms. This is of particular importance as SCRAs are usually smoked by consumers and hCES1 is
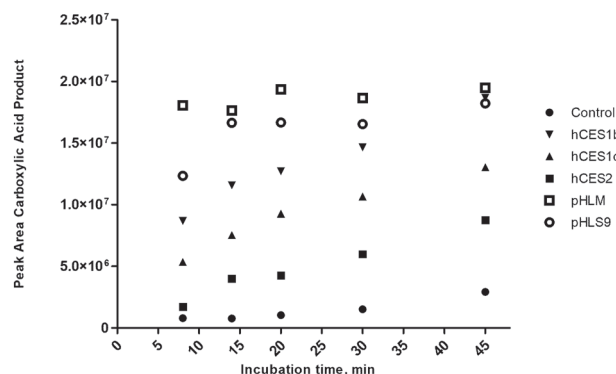
FIGURE 6 Results of carboxylesterases activity screening of quinolin-8-yl 4-methyl-3-((propan-2-yl)sulfamoyl)benzoate (QMiPSB): peak area of carboxylic acid hydrolysis product using different enzyme sources. Values from time point zero were subtracted from all the following time points. Shown data represent the mean of duplicate determination. hCES, human carboxylesterases; pHLM, pooled human liver microsomes; pHLS9, pooled human liver S9 fraction

the predominant isoform in the human lung.[24] Previous studies revealed that the hydrolysis of the related SCRAs QMPSB, 2F-QMPSB, BB-22, PB-22, and 5F-PB-22, which also have an 8-hydroxyquinoline ester head group, was mainly catalyzed by hCES1 as well.[12,13,25] Furthermore, a study on SCRAs containing a methyl ester showed that mostly hCES1 catalyzed the hydrolysis.[26]

Incubations with pHLM and pHLS9 revealed a faster increase in the hydrolysis product than the control incubations, indicating enzymatic ester hydrolysis as well. In both incubations, QMiPSB was almost completely degraded after 8 or 14 min, so no further ester hydrolysis was possible. These results show that the natural hCES spectrum of the human liver can cleave the ester bond of QMiPSB. Since hCES1 is predominantly expressed in the liver, this result is in agreement with the results of the recombinant esterases.[24] However, as the manufacturer of the pHLM and pHLS9 solutions does not specify any hCES activities, only qualitative statements are possible here.

These results indicate that ester hydrolysis plays an important role in the Phase I metabolism of QMiPSB and is mainly catalyzed by hCES1 isoforms. In addition to the enzymatic ester hydrolysis, nonenzymatic ester hydrolysis was observed, which further accelerates the ester hydrolysis. Therefore, mainly ester hydrolysis products and their metabolites can be expected in in vivo samples. The chemical instability of the ester bond must also be taken into account during sample storage and processing. No solvents leading to hydrolysis or transesterification should be used.

4 | CONCLUSIONS

A total of 15 QMMSB metabolites and 16 QMiPSB metabolites were tentatively identified by LC-HR-MS/MS in the in vitro incubations. The carboxylesterases activity assay showed that ester hydrolysis is an important step in the metabolism of the quinolin-8-yl ester head group,

whereby the ester bond of QMiPSB was cleaved primarily by hCES1 isoforms. For both substances, QMMSB and QMiPSB, the two ester hydrolysis products as well as their glucuronides are assumed to be the most important targets for toxicological plasma and urine screenings. Additional measurements in the negative ionization mode increase the detectability of the carboxylic acid products of ester hydrolysis and their metabolites. Several CYP isoforms are involved in the metabolism of QMMSB and QMiPSB, with both substances being metabolized by CYP2C8, CYP2C9, CYP3A4, and CYP3A5. The hepatic clearance of QMMSB and QMiPSB should therefore not be significantly impaired by a drug–drug interaction targeting a single CYP isozyme.

ORCID

Lea Wagmann 🄳 https://orcid.org/0000-0001-7470-7912
Simon D. Brandt 🄳 https://orcid.org/0000-0001-8632-5372
Markus R. Meyer 🄳 https://orcid.org/0000-0003-4377-6784

REFERENCES

1. UNODC. World Drug Report 2021 (United Nations publication, Sales No. E.21.XI.8). https://www.unodc.org/res/wdr2021/field/WDR21_Booklet_2.pdf. Accessed August 11, 2022.
2. Tait RJ, Caldicott D, Mountain D, Hill SL, Lenton S. A systematic review of adverse events arising from the use of synthetic cannabinoids and their associated treatment. *Clin Toxicol (Phila)*. 2016;54(1):1-13. doi:10.3109/15563650.2015.1110590
3. EMCDDA. European Drug Report 2022 - Trends and Developments. 2022. https://www.emcdda.europa.eu/system/files/publications/14644/TDAT22001ENN.pdf. Accessed August 11, 2022.
4. EMCDDA. Perspectives on drugs, Synthetic cannabinoids in Europe. 2017. https://www.emcdda.europa.eu/system/files/publications/2753/POD_Synthetic%20cannabinoids_0.pdf. Accessed August 11, 2022.
5. Lambeng N, Lebon F, Christophe B, Burton M, De Ryck M, Quere L. Arylsulfonamides as a new class of cannabinoid CB1 receptor ligands: identification of a lead and initial SAR studies. *Bioorg Med Chem Lett*. 2007;17(1):272-277. doi:10.1016/j.bmcl.2006.09.049
6. Ermann M, Riether D, Walker ER, et al. Arylsulfonamide CB2 receptor agonists: SAR and optimization of CB2 selectivity. *Bioorg Med Chem Lett*. 2008;18(5):1725-1729. doi:10.1016/j.bmcl.2008.01.042
7. Brandt SD, Kavanagh PV, Westphal F, et al. Synthetic cannabinoid receptor agonists: analytical profiles and development of QMPSB, QMMSB, QMPCB, 2F-QMPSB, QMiPSB, and SGT-233. *Drug Test Anal*. 2021;13(1):175-196. doi:10.1002/dta.2913
8. Blakey K, Boyd S, Atkinson S, et al. Identification of the novel synthetic cannabimimetic 8-quinolinyl 4-methyl-3-(1-piperidinylsulfonyl)benzoate (QMPSB) and other designer drugs in herbal incense. *Forensic Sci Int*. 2016;260:40-53. doi:10.1016/j.forsciint.2015.12.001
9. Tsochatzis ED, Alberto Lopes J, Holland MV, Reniero F, Palmieri G, Guillou C. Identification and analytical characterization of a novel synthetic cannabinoid-type substance in herbal material in Europe. *Molecules*. 2021;26(4):793. doi:10.3390/molecules26040793
10. Uchiyama N, Matsuda S, Kawamura M, Kikura-Hanajiri R, Goda Y. Two new-type cannabimimetic quinolinyl carboxylates, QUPIC and

QUCHIC, two new cannabimimetic carboxamide derivatives, ADB-FUBINACA and ADBICA, and five synthetic cannabinoids detected with a thiophene derivative α-PVT and an opioid receptor agonist AH-7921 identified in illegal products. *Forensic Toxicol*. 2013;31(2):223-240. doi:10.1007/s11419-013-0182-9

11. Wagmann L, Maurer HH. Bioanalytical methods for new psychoactive substances. *Handb Exp Pharmacol*. 2018;252:413-439. doi:10.1007/164_2017_83

12. Richter MJ, Wagmann L, Gampfer TM, Brandt SD, Meyer MR. In vitro metabolic fate of the synthetic cannabinoid receptor agonists QMPSB and QMPCB (SGT-11) including isozyme mapping and esterase activity. *Metabolites*. 2021;11(8):509. doi:10.3390/metabo11080509

13. Richter MJ, Wagmann L, Brandt SD, Meyer MR. In vitro metabolic fate of the synthetic cannabinoid receptor agonists 2F-QMPSB and SGT-233 including isozyme mapping and carboxylesterases activity testing. *J Anal Toxicol*. 2022;1-9. doi:10.1093/jat/bkac072

14. Richter LHJ, Flockerzi V, Maurer HH, Meyer MR. Pooled human liver preparations, HepaRG, or HepG2 cell lines for metabolism studies of new psychoactive substances? A study using MDMA, MDBD, butylone, MDPPP, MDPV, MDPB, 5-MAPB, and 5-API as examples. *J Pharm Biomed Anal*. 2017;143:32-42. doi:10.1016/j.jpba.2017.05.028

15. Wagmann L, Meyer MR, Maurer HH. What is the contribution of human FMO3 in the N-oxygenation of selected therapeutic drugs and drugs of abuse? *Toxicol Lett*. 2016;258:55-70. doi:10.1016/j.toxlet.2016.06.013

16. Helfer AG, Michely JA, Weber AA, Meyer MR, Maurer HH. Orbitrap technology for comprehensive metabolite-based liquid chromatographic-high resolution-tandem mass spectrometric urine drug screening - exemplified for cardiovascular drugs. *Anal Chim Acta*. 2015;891:221-233. doi:10.1016/j.aca.2015.08.018

17. Wagmann L, Manier SK, Felske C, et al. Flubromazolam-derived designer benzodiazepines: Toxicokinetics and analytical toxicology of Clobromazolam and Bromazolam. *J Anal Toxicol*. 2021;45(9):1014-1027. doi:10.1093/jat/bkaa161

18. Diao X, Scheidweiler KB, Wohlfarth A, Pang S, Kronstrand R, Huestis MA. In vitro and in vivo human metabolism of synthetic cannabinoids FDU-PB-22 and FUB-PB-22. *AAPS j*. 2016;18(2):455-464. doi:10.1208/s12248-016-9867-4

19. Holsztynska EJ, Domino EF. Biotransformation of phencyclidine. *Drug Metab Rev*. 1985;16(3):285-320. doi:10.3109/03602538508991437

20. Michely JA, Manier SK, Caspar AT, Brandt SD, Wallach J, Maurer HH. New psychoactive substances 3-Methoxyphencyclidine (3-MeO-PCP) and 3-Methoxyrolicyclidine (3-MeO-PCPy): metabolic fate elucidated with rat urine and human liver preparations and their detectability in urine by GC-MS, "LC-(high resolution)-MSn" and "LC-(high resolution)-MS/MS". *Curr Neuropharmacol*. 2017;15(5):692-712. doi:10.2174/1570159X14666161018151716

21. Meyer MR, Schutz A, Maurer HH. Contribution of human esterases to the metabolism of selected drugs of abuse. *Toxicol Lett*. 2015;232(1):159-166. doi:10.1016/j.toxlet.2014.10.026

22. Thomsen R, Rasmussen HB, Linnet K, The INDICES Consortium. In vitro drug metabolism by human carboxylesterase 1: focus on angiotensin-converting enzyme inhibitors. *Drug Metab Dispos*. 2014;42(1):126-133. doi:10.1124/dmd.113.053512

23. Wang J, Williams ET, Bourgea J, Wong YN, Patten CJ. Characterization of recombinant human carboxylesterases: fluorescein diacetate as a probe substrate for human carboxylesterase 2. *Drug Metab Dispos*. 2011;39(8):1329-1333. doi:10.1124/dmd.111.039628

24. Di L. The impact of carboxylesterases in drug metabolism and pharmacokinetics. *Curr Drug Metab*. 2019;20(2):91-102. doi:10.2174/1389200219666180821094502

25. Thomsen R, Nielsen LM, Holm NB, Rasmussen HB, Linnet K, the INDICES Consortium. Synthetic cannabimimetic agents metabolized by carboxylesterases. *Drug Test Anal*. 2015;7(7):565-576. doi:10.1002/dta.1731

26. Wagmann L, Stiller RG, Fischmann S, Westphal F, Meyer MR. Going deeper into the toxicokinetics of synthetic cannabinoids: in vitro contribution of human carboxylesterases. *Arch Toxicol*. 2022;96(10):2755-2766. doi:10.1007/s00204-022-03332-z

SUPPORTING INFORMATION

Additional supporting information can be found online in the Supporting Information section at the end of this article.